Supplement of Atmos. Chem. Phys., 22, 5033–5069, 2022
https://doi.org/10.5194/acp-22-5033-2022-supplement

Atmospheric Chemistry and Physics
Open Access

Supplement of

Aerosol optical properties calculated from size distributions, filter samples and absorption photometer data at Dome C, Antarctica, and their relationships with seasonal cycles of sources

Aki Virkkula et al.

Correspondence to: Aki Virkkula (aki.virkkula@fmi.fi)

SUPPLEMENT

Contents

1. Wind direction and speed analysis of contamination sector at the aerosol measurement site

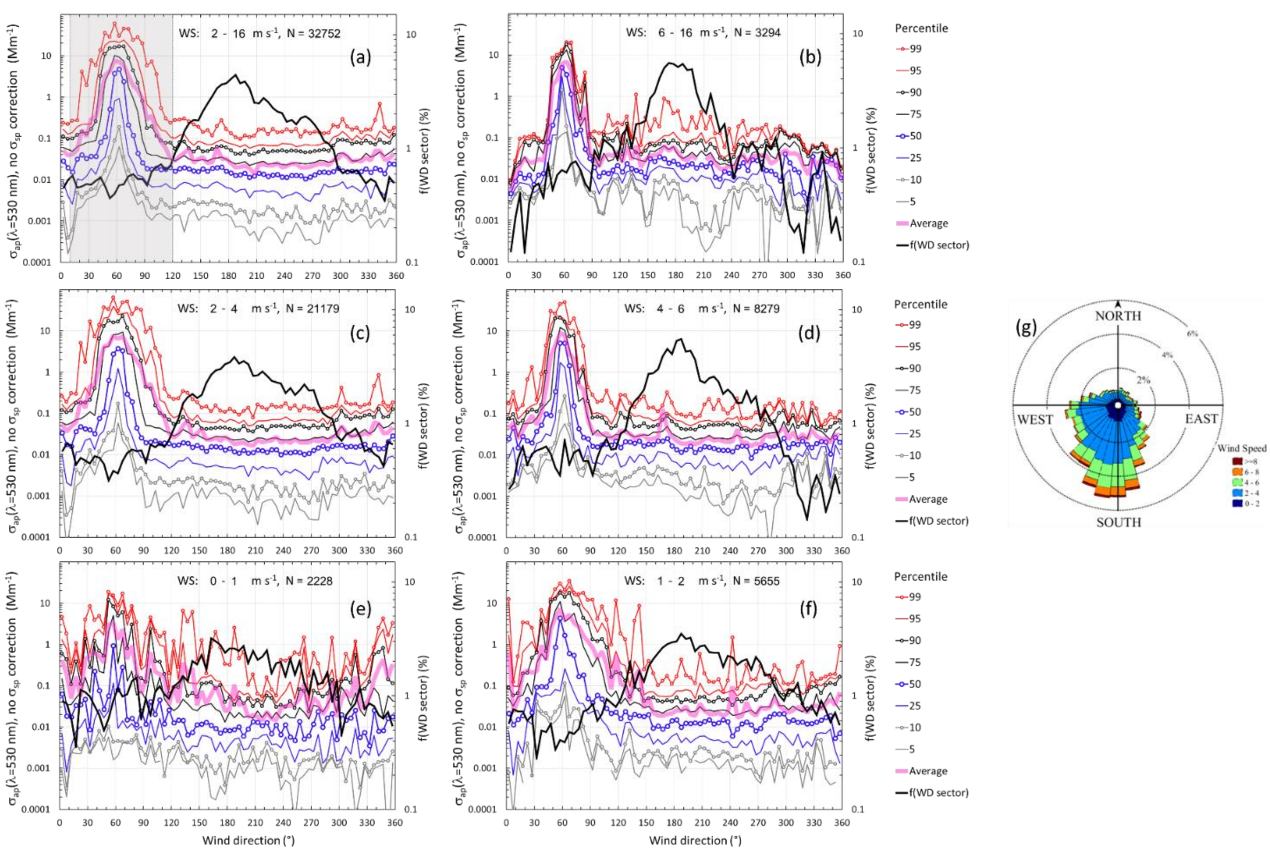

Figure S1. Wind and absorption coefficient. a) Hourly-averaged non-scattering-corrected absorption coefficients ($\sigma_{ap,nsc}$, Eq. (1)) in 5° wind direction (WD) sectors observed at six wind speed (WS) ranges: 0 – 1 m s^{-1}, 1 – 2 m s^{-1}, 2 – 4 m s^{-1}, 4 – 6 m s^{-1}, 6 – 16 m s^{-1}, and 2 – 16 m s^{-1}. The lines present the percentiles of the cumulative $\sigma_{ap,nsc}$ distribution in each WD sector. f(WD sector): fraction of wind data from each sector. CS 75th perc.: Contamination sector determined from the 75th percentiles of the cumulative $\sigma_{ap,nsc}$ distribution. CS 99th perc.: Contamination sector determined from the 99th percentiles of the cumulative $\sigma_{ap,nsc}$ distribution. g) Distribution of WS and WD as a wind rose.

2. Estimated wind speed and particle size dependent inlet and sampling line losses for large particles

The inlet was a straight 25 mm stainless steel tube with a protective cap. The cap extended about 2 cm below the top of the main inlet tube. For estimating the inlet and sample tube transmittances Paul A. Baron's aerosol calculator spreadsheet, AEROCALC was used. It is available at https://therealandrewmaynard.com/2020/05/27/the-aerosol-calculator/.

The equations used there are presented in Aerosol Measurement: Principles, Techniques, and Applications, Third Edition, Edited by P. Kulkarni, P. A. Baron, and K. Willeke, John Wiley & Sons, Inc., 2011. For the inlet type used here neither the book nor the Excel sheet presents any equations. Therefore an approximation was done by assuming that the inlet was the main inlet tube with a 180° turn downwards on the top of it. Consequently, sample air flows 2 cm upwards when it enters the inlet, just like in the actual inlet. Size-dependent transmittance $f_{inlet,tubing}(D_p)$ was calculated taking into account wind-speed-dependent inertial losses in a sharp-edged inlet and impaction losses in the inlet's 180° bend and one 90° bend from the inlet tube to the OPC inside the measurement container.

Fig. S2 shows example of the calculated inlet transmittances at five different wind speeds. The selected wind speeds are the 5th percentile (2.2 m s^{-1}), average (3.9 m s^{-1}), the 95th percentile (7.1 m s^{-1}), and the 99th percentile (9.3 m s^{-1}) of all wind speeds larger than 2 m s^{-1} observed at Dome C in 2008 – 2013. The monthly time series and seasonal cycles of wind speed are presented in Fig. S3 and Table SW1.

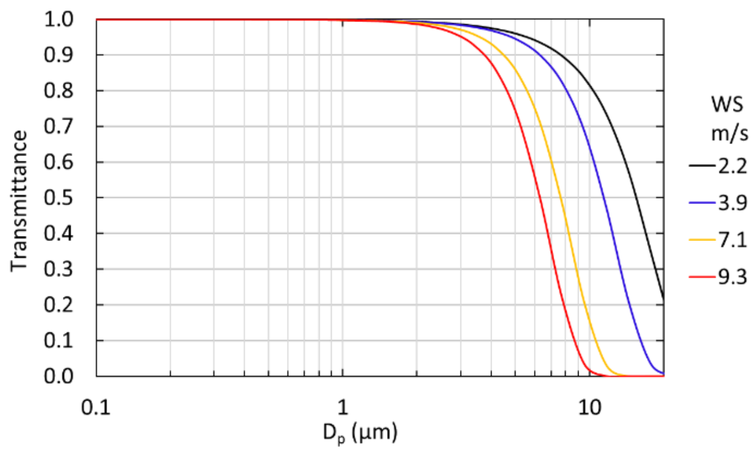

Figure S2. Examples of combined inlet and sampling tube transmittance taking into account wind-speed-dependent losses in the inlet and impaction losses between the inlet and the OPC.

The losses are negligible at D_p < 1 µm so the correction was done for supermicron particles only. The correction was simply a division by the transmittance:

$$n(D_p) = n(D_p, OPC, noncorrected) / f_{inlet,tubing}(WS, D_p) \quad (S1)$$

This correction was done for each hourly-averaged size distributions using the simultaneously measured wind speeds in December 2007 – July 2009.

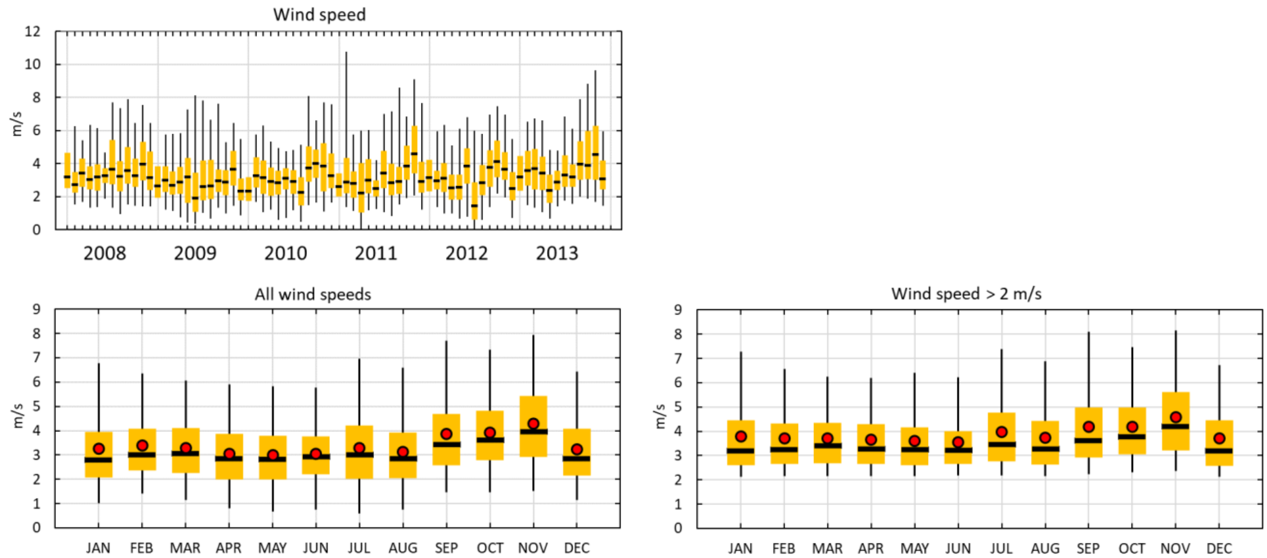

Figure S3. Wind speed at Dome C in 2008 – 2013. a) Monthly WS 5th ,25th, 50th , 75th and 95th percentiles, b) Seasonal cycle of wind speed. All data, monthly WS 5th ,25th, 50th , 75th and 95th percentiles and averages (red circle), c) Seasonal cycle of WS > 2 m s^{-1}. All data, monthly WS 5th ,25th, 50th , 75th and 95th percentiles and averages (red circle).

Table SW1. Descriptive statistics of wind speed at Dome C in 2008 – 2013. WS in m/s. The line WS > 2 m/s presents the statistics of the time when WS was high enough for avoiding contamination.

			PERCENTILES							
	N	ave ± std	5	10	25	50	75	90	95	99
ALL WS	51905	3.4 ± 1.8	1.0	1.5	2.3	3.1	4.2	5.7	6.8	9.1
WS > 2 m/s	42105	3.9 ± 1.6	2.2	2.3	2.7	3.4	4.6	6.0	7.1	9.3

ALL WS, m/s

			PERCENTILES				
	N	ave ± std	5	25	50	75	95
JAN	4389	3.3 ± 1.9	1.0	2.1	2.8	4.0	6.8
FEB	4046	3.4 ± 1.7	1.4	2.4	3.0	4.1	6.4
MAR	4421	3.3 ± 1.5	1.1	2.3	3.1	4.1	6.1
APR	4286	3.1 ± 1.6	0.8	2.0	2.8	3.9	5.9
MAY	4379	3.0 ± 1.6	0.7	2.0	2.8	3.8	5.8
JUN	4265	3.1 ± 1.5	0.7	2.2	2.9	3.8	5.8
JUL	4385	3.3 ± 1.9	0.6	2.0	3.0	4.2	7.0
AUG	4416	3.1 ± 1.7	0.8	2.0	2.8	3.9	6.6
SEP	4199	3.9 ± 2.0	1.5	2.6	3.4	4.7	7.7
OCT	4453	3.9 ± 1.7	1.5	2.8	3.6	4.8	7.3
NOV	4302	4.3 ± 2.0	1.5	2.9	4.0	5.4	7.9
DEC	4364	3.2 ± 1.6	1.1	2.2	2.8	4.1	6.4
ALL	51905	3.4 ± 1.8	1.0	2.3	3.1	4.2	6.8

WS > 2 m/s

			PERCENTILES				
	N	ave ± std	5	25	50	75	95
JAN	3414	3.8 ± 1.8	2.1	2.6	3.2	4.5	7.3
FEB	3464	3.7 ± 1.6	2.2	2.6	3.3	4.3	6.6
MAR	3620	3.7 ± 1.4	2.2	2.7	3.4	4.4	6.3
APR	3216	3.6 ± 1.4	2.1	2.6	3.3	4.3	6.2
MAY	3276	3.6 ± 1.4	2.2	2.6	3.3	4.2	6.4
JUN	3379	3.5 ± 1.3	2.2	2.7	3.2	4.0	6.2
JUL	3299	4.0 ± 1.6	2.2	2.8	3.5	4.8	7.4
AUG	3342	3.7 ± 1.5	2.2	2.6	3.3	4.4	6.9
SEP	3701	4.2 ± 1.9	2.2	2.9	3.6	5.0	8.1
OCT	4028	4.2 ± 1.6	2.3	3.0	3.8	5.0	7.5
NOV	3892	4.6 ± 1.8	2.4	3.2	4.2	5.6	8.1
DEC	3474	3.7 ± 1.5	2.1	2.6	3.2	4.4	6.7
ALL	42105	3.9 ± 1.6	2.2	2.7	3.4	4.6	7.1

3. Seasonal cycle tables of aerosol optical properties and mass concentrations at Dome C in 2008-2013

Table S1. Seasonal averages, 25th, 50th and 75th percentiles of mass concentrations calculated from the number size distributions (m(DMPS,$PM_{0.8}$) and m(DMPS,PM_{10})) and the sum of chemical constituents analyzed from the PM_1 and PM_{10} filter samples. N: for m(DMPS) the number of hourly data, for PM_1 and PM_{10} the number of filter samples. See the main text for detailed explanations.

m(size distributions)		m(DMPS,$PM_{0.8}$), ng m^{-3}				m(DMPS,PM_{10}), ng m^{-3}			
			Percentiles				Percentiles		
	N	AVE	25	50	75	AVE	25	50	75
JAN	1263	247	148	191	268	288	172	223	312
FEB	2480	299	174	272	386	351	204	320	454
MAR	1912	139	86	121	164	176	108	153	208
APR	1735	61	33	48	87	84	46	67	121
MAY	1880	42	17	26	37	78	32	48	69
JUN	1434	88	15	22	49	182	30	45	103
JUL	2471	85	17	32	57	176	35	66	119
AUG	1783	52	13	21	41	97	25	39	77
SEP	2021	72	33	49	71	117	53	80	115
OCT	2421	71	48	62	83	111	75	97	130
NOV	1275	151	94	122	208	204	127	165	282
DEC	1312	192	128	161	263	239	159	201	328
N_{tot}	21987								

m(filter samples)		PM_1, ng m^{-3}				PM_{10}, ng m^{-3}				
			Percentiles					Percentiles		
	N	AVE	25	50	75	N	AVE	25	50	75
JAN	45	141	82	141	183	159	167	111	143	208
FEB	41	179	116	172	238	161	235	143	194	287
MAR	45	92	66	88	114	183	164	93	138	207
APR	44	53	30	46	71	177	121	60	93	134
MAY	47	38	19	31	48	137	126	44	88	148
JUN	34	39	17	26	37	148	139	40	75	171
JUL	36	63	24	43	69	134	159	53	104	171
AUG	39	54	23	44	69	135	150	56	113	194
SEP	39	56	36	46	65	114	169	53	83	196
OCT	29	51	22	47	66	159	148	82	125	196
NOV	30	88	68	87	118	124	203	107	173	247
DEC	39	114	82	112	142	133	167	94	140	204
N_{tot}	468					1764				

Table S2. Seasonal averages, 25th, 50th and 75th percentiles of scattering coefficients calculated from the particle number size distributions (σ_{sp}(DMPS,$PM_{0.8}$) and σ_{sp}(DMPS,PM_{10})) at λ = 530 nm and from the filter samples (σ_{sp}(PM_1) and σ_{sp}(PM_{10})) at λ = 550 nm. See the main text for detailed explanations. Explanation of columns as in Table S1.

σ_{sp}(size distributions)		σ_{sp}(DMPS,$PM_{0.8}$), Mm^{-1}				σ_{sp}(DMPS,PM_{10}), Mm^{-1}			
			Percentiles				Percentiles		
	N	AVE	25	50	75	AVE	25	50	75
JAN	1263	0.43	0.17	0.29	0.44	0.55	0.22	0.37	0.57
FEB	2480	0.54	0.23	0.45	0.71	0.72	0.31	0.60	0.94
MAR	1912	0.23	0.14	0.20	0.32	0.33	0.20	0.29	0.46
APR	1735	0.13	0.05	0.10	0.15	0.19	0.08	0.15	0.23
MAY	1880	0.11	0.03	0.05	0.09	0.22	0.06	0.10	0.17
JUN	1434	0.30	0.03	0.06	0.14	0.60	0.07	0.12	0.28
JUL	2471	0.30	0.05	0.09	0.19	0.58	0.09	0.17	0.36
AUG	1783	0.16	0.04	0.06	0.12	0.28	0.06	0.10	0.20
SEP	2021	0.23	0.09	0.14	0.22	0.35	0.14	0.21	0.35
OCT	2421	0.18	0.10	0.15	0.21	0.27	0.16	0.23	0.33
NOV	1275	0.32	0.14	0.24	0.52	0.47	0.21	0.35	0.75
DEC	1312	0.31	0.19	0.25	0.42	0.44	0.27	0.34	0.58
N_{tot}	21987								

σ_{sp}(filter samples)		σ_{sp}(PM_1), Mm^{-1}				σ_{sp}(PM_{10}), Mm^{-1}				
			Percentiles					Percentiles		
	N	AVE	25	50	75	N	AVE	25	50	75
JAN	45	0.51	0.29	0.51	0.66	159	0.32	0.21	0.27	0.39
FEB	41	0.64	0.42	0.62	0.86	161	0.45	0.27	0.37	0.55
MAR	45	0.33	0.24	0.32	0.41	183	0.31	0.18	0.26	0.39
APR	44	0.19	0.11	0.17	0.26	177	0.23	0.11	0.18	0.26
MAY	47	0.14	0.07	0.11	0.17	137	0.24	0.08	0.17	0.28
JUN	34	0.14	0.06	0.09	0.13	148	0.26	0.08	0.14	0.32
JUL	36	0.23	0.09	0.16	0.25	134	0.30	0.10	0.20	0.33
AUG	39	0.19	0.08	0.16	0.25	135	0.28	0.11	0.22	0.37
SEP	39	0.20	0.13	0.16	0.23	114	0.32	0.10	0.16	0.37
OCT	29	0.18	0.08	0.17	0.24	159	0.28	0.16	0.24	0.37
NOV	30	0.32	0.24	0.31	0.43	124	0.39	0.20	0.33	0.47
DEC	39	0.41	0.30	0.40	0.51	133	0.32	0.18	0.27	0.39
N_{tot}	468					1764				

Table S3. Seasonal averages, 25th, 50th and 75th percentiles of scattering Ångström exponents of the wavelength pair λ = 467 nm and 660 nm calculated from the lower and upper estimates of scattering coefficients, (σ_{sp}(DMPS,$PM_{0.8}$) and σ_{sp}(DMPS,PM_{10}), respectively. See the main text for details. Unitless. Explanation of columns as in Table S1.

		α_{sp}(σ_{sp}(DMPS,$PM_{0.8}$))				α_{sp}(σ_{sp}(DMPS,PM_{10}))			
			Percentiles				Percentiles		
	N	AVE	25	50	75	AVE	25	50	75
JAN	1263	2.64	2.55	2.69	2.78	1.89	1.80	1.94	2.03
FEB	2480	2.62	2.55	2.63	2.76	1.89	1.81	1.89	2.02
MAR	1912	2.49	2.26	2.57	2.72	1.73	1.50	1.80	1.96
APR	1735	2.26	2.12	2.25	2.38	1.45	1.31	1.43	1.57
MAY	1880	2.24	2.11	2.24	2.36	1.17	1.03	1.16	1.29
JUN	1434	2.05	1.96	2.05	2.15	0.78	0.69	0.78	0.87
JUL	2471	2.09	1.98	2.05	2.16	0.88	0.77	0.85	0.95
AUG	1783	2.10	2.03	2.11	2.20	1.05	0.97	1.05	1.15
SEP	2021	2.08	1.98	2.11	2.21	1.19	1.08	1.21	1.31
OCT	2421	2.13	2.08	2.15	2.21	1.23	1.17	1.24	1.30
NOV	1275	2.27	2.15	2.31	2.43	1.34	1.22	1.38	1.50
DEC	1312	2.55	2.50	2.55	2.62	1.61	1.56	1.60	1.67
N_{tot}	21987								

Table S4. Seasonal averages, 25th, 50th and 75th percentiles of absorption coefficient. σ_{ap}(B1999, no σ_{sp} correction): σ_{ap} calculated by using Eq. (11) without scattering correction, essentially that calculated by the PSAP; $\sigma_{ap}(\sigma_{sp}(DMPS,PM_{10}),B1999)$: σ_{ap} calculated by using $\sigma_{sp}(DMPS,PM_{10})$ for the scattering correction in Eq. (11); $\sigma_{ap}(\sigma_{sp}(DMPS,PM_{10}),V2010)$: σ_{ap} calculated by using $\sigma_{sp}(DMPS,PM_{10})$ for the scattering correction in Eq. (12). Unit: Mm^{-1}.

σ_{ap} (λ=530 nm), Mm^{-1}													
	$\sigma_{ap,nsc}$					$\sigma_{ap}(\sigma_{sp}(DMPS,PM_{10}),B1999)$				$\sigma_{ap}(\sigma_{sp}(DMPS,PM_{10}),V2010)$			
			Percentiles				Percentiles				Percentiles		
	N	AVE	25	50	75	AVE	25	50	75	AVE	25	50	75
JAN	838	0.0212	0.0135	0.0175	0.0228	0.0118	0.0057	0.0103	0.0160	0.0105	0.0045	0.0086	0.0142
FEB	1756	0.0229	0.0125	0.0151	0.0236	0.0114	0.0030	0.0079	0.0142	0.0098	0.0017	0.0061	0.0125
MAR	1227	0.0110	0.0071	0.0100	0.0137	0.0051	0.0016	0.0037	0.0077	0.0043	0.0007	0.0028	0.0065
APR	1052	0.0073	0.0051	0.0064	0.0093	0.0038	0.0013	0.0028	0.0064	0.0035	0.0007	0.0024	0.0062
MAY	1262	0.0082	0.0024	0.0040	0.0073	0.0041	0.0008	0.0017	0.0046	0.0036	0.0006	0.0014	0.0041
JUN	1056	0.0143	0.0027	0.0046	0.0151	0.0047	0.0004	0.0017	0.0065	0.0040	0.0001	0.0016	0.0052
JUL	1886	0.0147	0.0047	0.0076	0.0139	0.0068	0.0012	0.0035	0.0073	0.0063	0.0007	0.0031	0.0064
AUG	1059	0.0145	0.0062	0.0102	0.0146	0.0101	0.0044	0.0069	0.0098	0.0091	0.0040	0.0061	0.0091
SEP	1681	0.0267	0.0119	0.0217	0.0289	0.0207	0.0086	0.0182	0.0255	0.0190	0.0076	0.0165	0.0236
OCT	1961	0.0287	0.0219	0.0260	0.0329	0.0243	0.0184	0.0227	0.0284	0.0227	0.0171	0.0213	0.0264
NOV	1091	0.0398	0.0233	0.0297	0.0578	0.0319	0.0170	0.0239	0.0494	0.0297	0.0153	0.0222	0.0469
DEC	946	0.0266	0.0176	0.0211	0.0257	0.0202	0.0127	0.0160	0.0200	0.0189	0.0119	0.0146	0.0185
N_{tot}	15815												

Table S5. Seasonal averages, 25th, 50th and 75th percentiles of single-scattering albedo.

Single-scattering albedo $\omega_o = \sigma_{sp}(DMPS,PM_{10})/(\sigma_{sp}(DMPS,PM_{10}) + \sigma_{ap})$, λ = 530 nm													
		$\omega_o(\sigma_{ap,nsc})$				$\omega_o(\sigma_{sp}(DMPS,PM_{10}),B1999)$				$\omega_o(\sigma_{sp}(DMPS,PM_{10}),V2010)$			
			Percentiles				Percentiles				Percentiles		
	N	AVE	25	50	75	AVE	25	50	75	AVE	25	50	75
JAN	838	0.953	0.935	0.958	0.972	0.968	0.950	0.974	0.988	0.971	0.954	0.977	0.990
FEB	1756	0.958	0.932	0.972	0.980	0.973	0.946	0.988	0.996	0.976	0.951	0.990	0.998
MAR	1227	0.964	0.959	0.974	0.980	0.980	0.975	0.990	0.996	0.982	0.978	0.992	0.998
APR	1052	0.952	0.943	0.960	0.979	0.966	0.958	0.976	0.995	0.968	0.960	0.978	0.997
MAY	1262	0.957	0.935	0.967	0.977	0.972	0.949	0.982	0.993	0.975	0.953	0.985	0.995
JUN	1056	0.963	0.950	0.967	0.982	0.977	0.965	0.982	0.998	0.980	0.967	0.984	1.000
JUL	1886	0.946	0.925	0.950	0.978	0.960	0.939	0.965	0.994	0.963	0.945	0.968	0.996
AUG	1059	0.912	0.873	0.914	0.961	0.926	0.886	0.928	0.977	0.931	0.894	0.934	0.980
SEP	1681	0.894	0.858	0.900	0.938	0.907	0.871	0.913	0.953	0.913	0.880	0.921	0.959
OCT	1961	0.890	0.863	0.897	0.918	0.903	0.876	0.911	0.932	0.909	0.883	0.916	0.938
NOV	1091	0.911	0.894	0.922	0.940	0.925	0.908	0.937	0.954	0.930	0.915	0.941	0.958
DEC	946	0.933	0.924	0.938	0.949	0.947	0.938	0.952	0.964	0.951	0.941	0.956	0.966
N_{tot}	15815												

Table S6. Seasonal averages, 25th, 50th and 75th percentiles of absorption Ångström exponent.

$\alpha_{ap}(\sigma_{ap} > 3 \times \delta\sigma_{ap})$															
	$\alpha_{ap}(\sigma_{ap,nsc})$					$\alpha_{ap}(\sigma_{sp}(DMPS,PM_{10}),B1999)$					$\alpha_{ap}(\sigma_{sp}(DMPS,PM_{10}),V2010)$				
			Percentiles					Percentiles					Percentiles		
	N	AVE	25	50	75	N	AVE	25	50	75	N	AVE	25	50	75
JAN	835	0.90	0.78	0.89	1.07	695	0.46	0.15	0.40	0.77	620	1.32	1.08	1.32	1.53
FEB	1743	0.93	0.50	0.82	1.22	983	0.85	0.34	0.83	1.51	870	1.18	0.78	1.21	1.50
MAR	1217	0.70	0.35	0.60	1.04	645	0.34	-0.27	0.37	0.94	530	1.29	0.70	1.45	1.66
APR	1045	0.69	0.50	0.69	0.84	529	0.56	0.38	0.52	0.99	494	1.36	1.22	1.34	1.49
MAY	1208	0.75	0.50	0.78	0.99	535	0.82	0.60	0.89	1.03	392	1.45	1.26	1.45	1.76
JUN	1044	0.80	0.60	0.79	0.97	429	0.94	0.61	0.90	1.27	262	1.71	1.24	1.61	2.24
JUL	1832	0.90	0.73	0.91	1.09	1180	0.88	0.64	0.90	1.12	917	1.56	1.47	1.64	1.79
AUG	1028	0.96	0.82	0.96	1.10	913	0.94	0.78	0.96	1.13	760	1.47	1.20	1.49	1.77
SEP	1668	0.93	0.86	0.96	1.04	1589	0.88	0.79	0.92	1.02	1472	1.42	1.24	1.42	1.60
OCT	1952	0.89	0.81	0.90	0.98	1952	0.84	0.73	0.84	0.95	1945	1.36	1.18	1.34	1.51
NOV	1089	0.87	0.79	0.89	0.95	1089	0.76	0.67	0.80	0.87	1062	1.38	1.23	1.35	1.49
DEC	946	0.83	0.72	0.84	0.92	936	0.55	0.42	0.60	0.75	946	1.30	1.13	1.27	1.43
N_{tot}	15607					11475					10270				

Table S7. Seasonal averages, 25th, 50th and 75th percentiles of equivalent Black Carbon concentrations calculated from the absorption coefficients at λ=530 nm calculated by using the B1999 algorithm without any scattering corrections and with B1999 and V2010 algorithms using σ_{sp} = σ_{sp}(DMPS,PM_{10}) for the scattering corrections and assuming MAC = 7.78 $m^2\ g^{-1}$.

eBC, ng m^{-3}													
		eBC($\sigma_{ap,nsc}$)				eBC(σ_{ap}(σ_{sp}(DMPS,PM_{10})), B1999)				eBC(σ_{ap}(σ_{sp}(DMPS,PM_{10})), V2010)			
			Percentiles				Percentiles				Percentiles		
	N	AVE	25	50	75	AVE	25	50	75	AVE	25	50	75
JAN	838	2.72	1.73	2.25	2.93	1.51	0.73	1.33	2.05	1.35	0.58	1.11	1.83
FEB	1756	2.95	1.60	1.94	3.03	1.46	0.39	1.02	1.82	1.26	0.22	0.78	1.61
MAR	1227	1.41	0.91	1.29	1.76	0.66	0.20	0.48	0.98	0.55	0.09	0.36	0.84
APR	1052	0.94	0.66	0.82	1.19	0.49	0.17	0.36	0.83	0.44	0.09	0.31	0.80
MAY	1262	1.06	0.30	0.52	0.93	0.53	0.11	0.21	0.59	0.47	0.07	0.17	0.53
JUN	1056	1.84	0.34	0.59	1.94	0.61	0.05	0.22	0.83	0.51	0.01	0.20	0.67
JUL	1886	1.89	0.61	0.98	1.79	0.87	0.15	0.45	0.93	0.81	0.09	0.40	0.83
AUG	1059	1.87	0.80	1.31	1.87	1.29	0.57	0.89	1.26	1.17	0.51	0.78	1.18
SEP	1681	3.43	1.54	2.79	3.71	2.66	1.10	2.34	3.27	2.44	0.98	2.12	3.03
OCT	1961	3.69	2.82	3.35	4.23	3.12	2.37	2.91	3.65	2.91	2.20	2.74	3.40
NOV	1091	5.11	2.99	3.81	7.43	4.10	2.18	3.07	6.34	3.81	1.97	2.85	6.03
DEC	946	3.42	2.26	2.71	3.30	2.60	1.63	2.06	2.57	2.42	1.53	1.88	2.38
N_{tot}	15815												

Table S8. Seasonal averages, 25th, 50th and 75th percentiles of mass fractions of equivalent Black Carbon concentrations calculated from (eBC/m(DMPS,$PM_{0.8}$))×100%.

eBC mass fraction: eBC/m(DMPS,$PM_{0.8}$), %													
		feBC($\sigma_{ap,nsc}$)				feBC(σ_{ap}(σ_{sp}(DMPS,PM_{10})), B1999)				feBC(σ_{ap}(σ_{sp}(DMPS,PM_{10})), V2010)			
			Percentiles				Percentiles				Percentiles		
	N	AVE	25	50	75	AVE	25	50	75	AVE	25	50	75
JAN	838	1.16	0.80	1.10	1.42	0.74	0.36	0.67	1.03	0.66	0.28	0.59	0.94
FEB	1756	1.19	0.64	0.90	1.39	0.71	0.14	0.38	1.05	0.63	0.08	0.30	0.95
MAR	1227	1.03	0.63	0.93	1.22	0.53	0.12	0.35	0.72	0.45	0.06	0.27	0.63
APR	1052	1.87	0.88	1.53	2.39	1.24	0.15	0.91	1.76	1.16	0.08	0.81	1.68
MAY	1262	2.38	1.25	1.74	3.54	1.50	0.38	0.87	2.76	1.35	0.26	0.73	2.57
JUN	1056	2.76	1.40	2.29	3.28	1.62	0.16	1.20	2.26	1.47	0.03	1.06	2.10
JUL	1886	3.66	1.69	3.75	5.11	2.57	0.44	2.61	4.06	2.32	0.29	2.30	3.65
AUG	1059	5.62	2.68	5.70	7.90	4.63	1.59	4.69	7.04	4.24	1.37	4.29	6.48
SEP	1681	6.33	3.87	5.78	7.74	5.41	2.87	4.97	6.99	5.04	2.54	4.47	6.41
OCT	1961	5.89	4.41	5.68	7.13	5.09	3.64	4.82	6.35	4.76	3.37	4.55	5.95
NOV	1091	3.68	2.48	3.08	4.88	3.04	1.79	2.44	3.96	2.82	1.60	2.31	3.75
DEC	946	1.98	1.50	1.85	2.42	1.53	1.06	1.39	1.95	1.42	0.97	1.28	1.75
N_{tot}	15815												

Table S9. Seasonal averages, 25th, 50th and 75th percentiles of mass fractions of equivalent Black Carbon concentrations calculated from (eBC/m(DMPS,PM_{10}))×100%.

eBC mass fraction: eBC/m(DMPS,PM_{10}), %													
		feBC($\sigma_{ap,nsc}$)				feBC(σ_{ap}(σ_{sp}(DMPS,PM_{10})), B1999)				feBC(σ_{ap}(σ_{sp}(DMPS,PM_{10})), V2010)			
			Percentiles				Percentiles				Percentiles		
	N	AVE	25	50	75	AVE	25	50	75	AVE	25	50	75
JAN	838	0.99	0.69	0.94	1.21	0.63	0.31	0.58	0.88	0.57	0.24	0.51	0.80
FEB	1756	1.01	0.54	0.77	1.18	0.61	0.12	0.33	0.90	0.54	0.06	0.26	0.81
MAR	1227	0.81	0.50	0.73	0.97	0.42	0.10	0.28	0.57	0.36	0.05	0.21	0.50
APR	1052	1.35	0.63	1.11	1.73	0.90	0.11	0.66	1.27	0.84	0.06	0.59	1.21
MAY	1262	1.28	0.67	0.94	1.90	0.81	0.20	0.47	1.48	0.73	0.14	0.39	1.38
JUN	1056	1.33	0.67	1.10	1.58	0.78	0.08	0.58	1.09	0.71	0.01	0.51	1.01
JUL	1886	1.77	0.82	1.82	2.47	1.24	0.21	1.26	1.97	1.12	0.14	1.11	1.77
AUG	1059	3.01	1.43	3.05	4.22	2.48	0.85	2.51	3.77	2.27	0.73	2.30	3.47
SEP	1681	3.91	2.39	3.58	4.78	3.35	1.78	3.08	4.32	3.12	1.57	2.77	3.96
OCT	1961	3.75	2.81	3.62	4.54	3.25	2.32	3.07	4.05	3.03	2.15	2.90	3.79
NOV	1091	2.72	1.83	2.28	3.61	2.25	1.33	1.81	2.93	2.09	1.19	1.71	2.77
DEC	946	1.59	1.21	1.49	1.95	1.23	0.85	1.12	1.56	1.14	0.78	1.03	1.41
N_{tot}	15815												

Table S10. Seasonal cycles of emissions of major absorbing and scattering aerosols.

BC emission:s Southern Hemisphere emissions from GFED v3.1data base (http://www.globalfiredata.org),
SSA: Sea-Spray Aerosol flux from the Southern Ocean, Grythe et al. (2014)

	BC emissions, g m^{-2}			SSA
Month	South America	Africa	Oceania	flux, g m^{-2} s^{-1}
JAN	4.9	3.1	8.9	0.924
FEB	6.1	2.1	5.2	1.227
MAR	7.4	2.8	2.0	1.253
APR	7.1	10.1	8.2	1.417
MAY	9.6	72.2	20.6	1.534
JUN	19.1	195.8	16.7	1.475
JUL	56.4	278.9	23.3	1.691
AUG	347.1	356.4	60.0	1.565
SEP	342.9	302.9	94.6	1.565
OCT	57.5	115.1	122.0	1.306
NOV	17.0	16.5	54.0	1.306
DEC	6.8	4.5	23.9	1.056